URSI AP-RASC 2019, New Delhi, India; 09 - 15 March 2019

Open Ended Microstrip-line-fed Compact Wideband MIMO-Diversity Antenna with Multiple Asymmetric Elliptical Wide-Slots

Munish Kumar[†], and Vandana Nath[*]
[†,*]University School of Information, Communication and Technology,
[†,*]Guru Gobind Singh Indraprastha University, Dwarka, New Delhi, 110078
[†]munishkm1989@gmail.com, [*]vandanausit@gmail.com

Abstract

This paper presents a compact, multiple-input-multiple-output (MIMO) microstrip-line-fed wide-slot antenna with good isolation for wideband applications. The proposed antenna consists of a large wide-slot formed by four asymmetric elliptical wide-slots (AEWSs) of different dimensions. These AEWSs when merged together, give the wideband response of 7.71 GHz (5.77-13.48 GHz; 80.1%) and good isolation with $|S_{21}| <$ -20 dB. The peak gain and maximum radiation efficiency of 8.66 dB and 88.58% respectively are obtained within the passband. The proposed antenna shows good diversity performance in terms of exceptionally low envelope correlation coefficient (<0.003) and low capacity loss of 0.12. Also, the maximum multiplexing efficiency of 88.56% (or -1.05 dB) along with total active reflection coefficient below 0 dB are reported in the entire frequency band. The proposed MIMO antenna has compact overall dimensions of 22×24 mm^2 that makes it a suitable candidate for modern handheld and portable wireless devices.

1 Introduction

Wideband multiple-input-multiple-output (MIMO) antenna systems are gaining much attention from antenna researchers due to their high transmission capacity without much increasing the power level. Two major factors that affect the diversity performance of a MIMO antenna system are mutual coupling between antenna elements and their overall size. Various techniques to obtain large impedance bandwidth (IBW) in MIMO antenna systems have been proposed. By introducing modifications in the radiating geometry either by merging two or more different shapes or tapering may lead to the generation of large impedance bandwidth. In [1], two circular monopole antennas with eye-shaped slot have been reported for ultra-wideband (UWB) range. In [2], the radiating patch consists of a semi-circle and rectangle shapes and is fed using a tapered microstrip line. In [3], two semi-circular stepped monopoles which are 90° angularly spaced have been used for obtaining wide IBW. A hybrid shape consisting of two semi-circles placed one over the other (in face-to-face) configuration is proposed in [4] shows exceptionally large IBW. Another way to modify the radiating geometry is to apply fractalization process to their edges as discussed in [5]. To minimize the overall dimensions, the radiating patch is cut by half (as per symmetry). In [6], a half cut CPW-fed circular antenna has been proposed for UWB operation. Another four elements CPW-fed half-cut elliptical shaped patch MIMO antenna for WLAN/LTE/UWB applications is discussed in [7]. Wide-slot antenna (having slot dimensions and operating wavelength are nearly same) structures are well known for their high gain and wideband behaviour. Wide-slot structures of various shapes such as hexagonal [8], rotated square [9], stepped rectangular [10], modified trapezoidal [11] have been already proposed for wideband applications.

Although the aforementioned antenna structures fulfil the bandwidth expectation but are larger in size and complex to design. Here, a two-element MIMO antenna having identical asymmetric elliptical wide-slots (AEWSs) excited by identical open-ended microstrip lines is proposed for wideband operation. The wideband operation of an antenna is attained by merging four AEWSs where each ellipse corresponds to a different operating frequency and hence, together give the wideband behaviour. Further, a rectangular slot is made in between the two AEWSs to increase the isolation between the two ports. The designed antenna is highly compact as compared to previous work on two-element wideband MIMO antennas. Details of obtaining the proposed antenna geometry and its analysis using accurate design equations are discussed in Section-2. Discussion of simulation results is performed in Section-3. Final inference is discussed in the conclusion section.

2 Antenna Design and Equivalent Circuit

2.1 Basic Geometry

Fig. 1 illustrates the geometry of the proposed wideband antenna, consisting of two identical AEWSs excited by two identical 50Ω impedance open-ended microstrip lines. The length of the microstrip line is divided into two parts: (l_1), having metallic ground plane beneath it and (l_2) not having

ground plane beneath it. As it can be seen that each AEWS

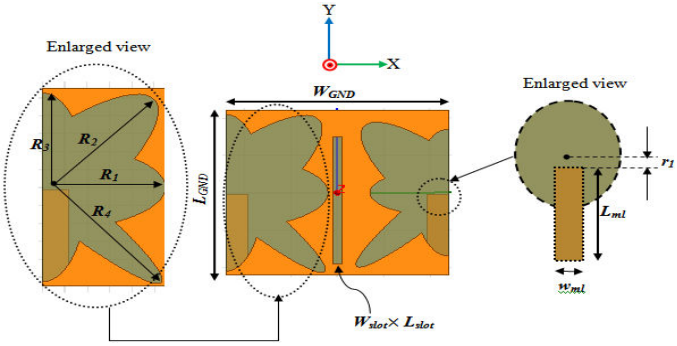

Figure 1. Schematic of the proposed antenna having two identical open-ended microstrip lines and AEWSs.

consists of four ellipses of semi-major axis R_1, R_2, R_3 and R_4. The resonant frequency of an EWS using approximated Mathieu function, q is given by [12]

$$f_{11}^{e,o} = \frac{15}{\pi e a}\sqrt{\frac{q_{11}^{e,o}}{\varepsilon_{rs}}} \quad \text{GHz} \tag{1}$$

where $f_{11}^{e,o}$ is the dual-frequency corresponding to TM_{11}^{e} and TM_{11}^{o} mode respectively. The approximated Mathieu function $q_{11}^{e,o}$ for even and odd mode are given in [12]. The feeding distance r_1 (shown in enlarged view of Fig. 1) plays a major role in impedance matching over a wide range of frequencies. To enhance the isolation between the two ports, a rectangular slot of dimensions $W_{slot} \times L_{slot}$ is placed between the AEWSs. The structure is simulated on ANSYS Electronics Desktop (version 17.0) using FR-4 substrate with ε_r=4.4, h=1.6 mm and loss tangent $tan\delta$=0.02. The overall dimensions of the antenna are 22×24 mm^2.

2.2 Equivalent Circuit

The equivalent circuit of the proposed antenna geometry is shown in Fig. 2 where Z_1 and Z_2 are the impedances due to lengths l_1 and l_2, respectively. The impedance Z_P and Z_f arise due to the coupling between microstrip line and AEWS and open ended microstrip line, respectively. The impedance Z'_{slot} is the impedance due to AEWS that depends on its dimensions. The expression of each impedance

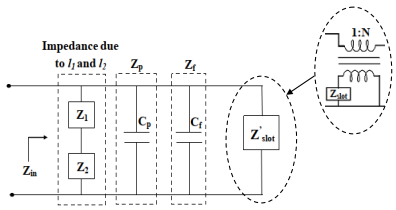

Figure 2. Equivalent circuit of an antenna with microstrip line and wide-slot.

shown in Fig. 2 along with detailed explanation is discussed in [13].

3 Results and Discussion

3.1 S_{11}, S_{21} and Impedance Parameters

The reflection coefficient S_{11} (in dB) for the proposed antenna is shown in Fig. 3(a). It can be seen that two frequency bands having S_{11} <-10 dB ranging from 4.61-4.98 GHz (f_r=4.83 GHz) and 5.77-13.48 GHz (f_r=7.85 GHz) are obtained. The level of isolaiton (S_{21}) is below -20 dB in both frequency bands which is acceptable for good performance of MIMO systems.

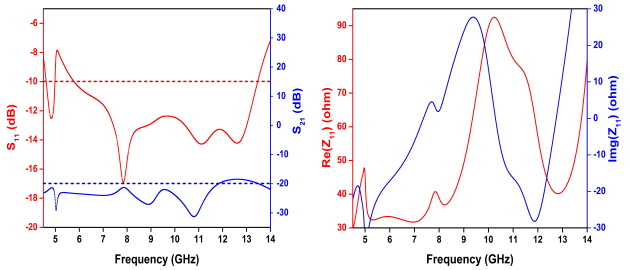

(a)

Figure 3. Simulated curve for (a) S_{11}/S_{21} (in dB) and (b) input impedance with respect to frequency of the proposed antenna.

Fig. 3(b) shows the variations of real and imaginary parts of the impedance with frequency. It is clear that the real oscillate around 50Ω with maximum and minimum values of 29.42Ω and 92.49Ω, respectively. Similarly, imaginary parts of the impedance oscillate around 0Ω with maximum and minimum values of -36.24Ω and 37.31Ω, respectively. The average magnitude of impedance over entire frequency band is 54.27Ω. Also, an impedance close to 50Ω is obtained at 4.83 and 7.85 GHz.

3.2 MIMO Performance

The performance of any MIMO antenna system is calculated in terms of envelope correlation coefficient (ECC), apparent diversity gain (ADG), mean effective gain (MEG), total active reflection coefficient (TARC) and MIMO voltage-standing-wave-ratio (MIMO-VSWR). The ECC parameter gives an idea of the level of mutual coupling between the adjacent antenna elements and can be given as [1]

$$\rho_e = |\rho_{i,j}|^2 = \frac{|S_{ii}^* S_{ij} + S_{ji}^* S_{jj}|^2}{(1-|S_{ii}|^2-|S_{ji}|^2)(1-|S_{jj}|^2-|S_{ij}|^2)}. \tag{2}$$

The ideal value of ECC is zero, but practically its value $\ll$ 0.5 is acceptable for an uncorrelated MIMO antenna system. Similarly ADG, a closely related parameter to ECC can be computed by using [1]

$$DG = 10\sqrt{1-|\rho_{i,j}|^2}. \quad (3)$$

Fig. 4(a) shows the simulated graph for ECC and DG which are less than 0.003 and more than 9.99 dB, respectively.

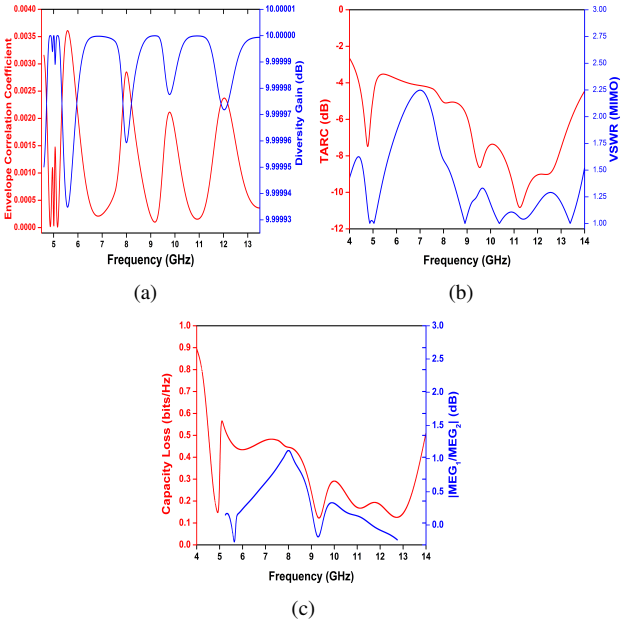

(a) (b) (c)

Figure 4. Diversity parameters (a) ECC/DG, (b) TARC/VSWR[MIMO], and (c) CCL/MEG for the proposed antenna.

When more than one antenna work simultaneously (as in case of MIMO antenna system), they start affecting the performance of each other. Hence, S-parameters cannot completely predict the actual behaviour of the system. Hence, another figure of merit known as TARC is introduced which is defined as the square root of the ratio of power reflected by the antenna to the total power incident and apparent return loss of the MIMO system which is given by [1]

$$TARC = \sqrt{\frac{(S_{11}+S_{12})^2+(S_{21}+S_{22})^2}{2}}. \quad (4)$$

Corresponding to TARC, the value of VSWR for a MIMO antenna system is calculated using

$$VSWR\,[MIMO] = \frac{1+TARC}{1-TARC}. \quad (5)$$

For an efficient MIMO antenna system, the TARC and VSWR[MIMO] should be below 0 dB and 2, respectively. For the proposed MIMO antenna, their value is below -6 dB and 2 for the entire frequency band, respectively as shown in Fig. 4(b). Another critical parameter for characterizing a MIMO system is MEG which is defined as the ratio of mean received power to the mean incident power, given by

$$MEG_i = 0.5\eta_{i,rad} = 0.5[1-\sum_{j=1}^{M}|S_{ij}|^2] \quad (6)$$

The loss of capacity in a MIMO antenna system due to correlation between antenna elements termed as the capacity loss and is given by

$$CCL = -log_2|\psi^R| \quad (7)$$

where ψ^R is a 2×2 correlation matrix whose elements are represented as

$$\psi^R = \begin{bmatrix} \rho_{11} & \rho_{12} \\ \rho_{21} & \rho_{22} \end{bmatrix}$$

Here, ρ_{ii}=$(1-|S_{ii}|^2-|S_{ij}|^2)$ and ρ_{ij}=$-(S^*_{ii}S_{ij}+S^*_{ji}S_{ij})$ for i,j=1 or 2. To full-fill the criteria of an efficient MIMO antenna system, $|\frac{MEG_i}{MEG_j}| < \pm 3$ dB and CCL< 0.4 bits/sec/Hz. From Fig. 4(c), it is clear that both ECC and CCL are within their limits required for wideband applications.

3.3 Radiation Performance

The 2-D radiation pattern at resonating frequencies 4.83 and 7.85 GHz are shown in Fig. 5(a) and (b), respectively. An omnidirectional radiation pattern due to back radiation is obtained at both lower and upper resonating frequencies. The back radiation can be minimized by putting a metallic reflector beneath the ground plane.

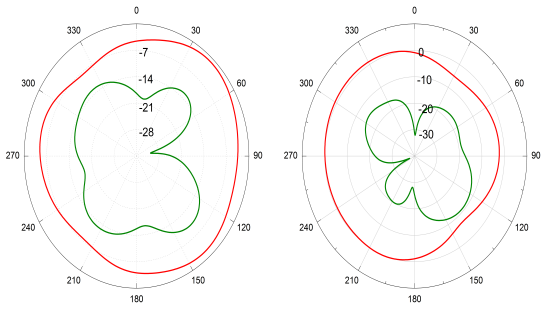

(a) (b)

Figure 5. Measured 2-D radiation pattern at (a) 4.83 GHz and (b) 7.85 GHz of the proposed antenna.

Fig. 6(a) shows the gain and radiation efficiency versus freqeuncy of the proposed antenna. The gain of the proposed antenna varies from 0.01 to 8.66 dB along with maximum efficiency of 98.57% in both frequency bands. While simulation, it has been observed that the efficiency of both the antennas due to symmetry remain almost same in the entire operating band. The absolute efficiency of a MIMO system can be characterized by using a parameter known as multiplexing efficiency (η_{MUX}) as shown in Fig. 6(b). It is the ratio of the required signal to noise ratio of the antenna under test (AUT/proposed) and isotropic antenna which can be approzimated as follows

$$\eta_{MUX} = \sqrt{(1-|\rho_{i,j}|^2)\eta_1\eta_2}. \quad (8)$$

where η_1 and η_2 are the total efficiency for the first and second antenna element. The multiplexing efficiency not only

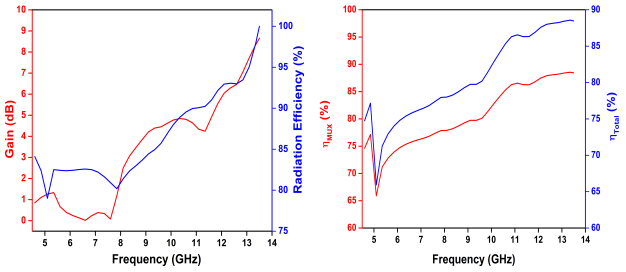

(a) (b)

Figure 6. (a) Gain and raidation efficiency and (b) total and multiplexing efficiencies versus frequency of the proposed antenna.

considers the total efficiency but also considers the correlation and efficiency imbalance. The maximum value multiplexing efficiency of 88.577% is obtained for the proposed MIMO antenna system.

4 Conclusion

An open-ended microstrip line fed wide-slot MIMO antenna with wideband characteristic is proposed. The proposed antenna achieves the operating bandwith ranging from 5.77-13.48 GHz with an isolation below -20 dB in the entire passband, by simply using a rectangular slot. With its wide bandwidth, compact dimensions (22×24 mm^2), stable radiation patterns and good diversity performance, the proposed MIMO antenna cut backs the need of using multiple antennas in wireless devices for accessing multiple applications.

References

[1] R. Chandel, A. K. Gautam and K. Rambabu, "Design and Packaging of an Eye-Shaped Multiple-Input-Multiple-Output Antenna With High Isolation for Wireless UWB Applications," *IEEE Trans. Comp. Pack. Manufac. Technol.*, **8**, 4, pp. 635–642, 2018.

[2] D. Yadav, M. P. Abegaonkar, S. K. Koul, V. Tiwari, and Deepak Bhatnagar, "Two Element Band-Notched UWB MIMO Antenna with High and Uniform Isolation," *Prog. Electromag. Res. M*, **63**, pp. 119–129, 2018.

[3] N. Jaglan, S. D. Gupta, E. Thakur, D. Kumar, B. K. Kanaujia, and S. Srivastava, "Triple Band Notched Mushroom and Uniplanar EBG Structures based UWB MIMO/Diversity Antenna with Enhanced Wide band Isolation," *AEU-Int. J. Electron. Commun.*, **90**, pp. 36–44, 2018.

[4] M. A. Ul Haq and S. Koziel, "Ground Plane Alterations for Design of High-Isolation Compact Wideband MIMO Antenna," *IEEE Access*, **6**, pp. 48978-48983, 2018.

[5] S. Tripathi, A. Mohan, and S. Yadav, "Performance Study of a Fractal UWB MIMO Antenna for On-body WBAN Applications," *Analog Integr Circ Sig Process*, **95**, 2, pp. 249–258, May 2018, doi: 10.1007/s10470-018-1138-0

[6] G. Liu, Y. Liu, and S. Gong, "Compact Uniplanar UWB MIMO Antenna with Band-notched Characteristic," *Microw. Opt. Technol. Lett.*, **59**, pp. 2207–2212, 2017.

[7] B. Yang, M. Chen, and L. Li, "Design of a Four-element WLAN/LTE/UWB MIMO Antenna using Half-slot Structure," *AEU-Int. J. Electron. Commun.*, **93**, pp. 354–359, 2018.

[8] S. Saxena, B. K. Kanaujia, S. Dwari, S. Kumar and R. Tiwari, "A Compact Dual-Polarized MIMO Antenna With Distinct Diversity Performance for UWB Applications," *IEEE Ant. Wirel. Propag. Lett.*, **16**, pp. 3096–3099, 2017.

[9] G. Irene and A. Rajesh, "A Dual-polarized UWB-MIMO Antenna with IEEE 802.11ac Band-notched Characteristics using Split-ring Resonator," *J. Comput. Electron.*, **17**, 3, pp. 1090–1098, 2018.

[10] M. A. Layegh, C. Ghobadi, J. Nourinia, Y. Samoodi, and S. N. Mashhadi, "Adaptive Neuro-Fuzzy Inference System approach in bandwidth and mutual coupling analyses of a novel UWB MIMO antenna with notch bands applicable for massive MIMOs," *AEU-Int. J. Electron. Commun.*, **94**, pp. 407–417, 2018.

[11] R. Devi and D. K. Neog, "A Compact Elevated CPW-fed Antenna with Slotted Ground Plane for Wideband Applications," *Int. J. Microw. Wirel. Technol.*, **9**, 10, pp. 2005–2011, 2017.

[12] J. G. Kretzschmar, "Wave Propagation in Hollow Conducting Elliptical Waveguides," in *IEEE Trans. Microw. Th. Tech.*, vol. 18, no. 9, pp. 547-554, Sep 1970.

[13] M. Kumar and V. Nath, "Microstrip-line-fed Elliptical Wide-slot Antenna with Similar Parasitic Patch for Multiband Applications," *IET Microw. Ant. Propag.*, August 2018, doi: 10.1049/iet-map.2018.5377